

# Re-examining the Solar Axion Explanation for the XENON1T Excess

Christina Gao,<sup>1</sup> Jia Liu,<sup>2</sup> Lian-Tao Wang,<sup>2,3</sup> Xiao-Ping Wang,<sup>4</sup> Wei Xue,<sup>5</sup> and Yi-Ming Zhong<sup>6</sup>

<sup>1</sup>*Theoretical Physics Department, Fermi National Accelerator Laboratory, Batavia, IL, 60510, USA*

<sup>2</sup>*Enrico Fermi Institute, University of Chicago, Chicago, IL 60637, USA*

<sup>3</sup>*Department of Physics, University of Chicago, Chicago, IL 60637, USA*

<sup>4</sup>*HEP Division, Argonne National Laboratory, 9700 Cass Ave., Argonne, IL 60439, USA*

<sup>5</sup>*Department of Physics, University of Florida, Gainesville, FL 32611, USA*

<sup>6</sup>*Kavli Institute for Cosmological Physics, University of Chicago, Chicago, IL 60637, USA*

The XENON1T collaboration has observed an excess in electronic recoil events below 5 keV over the known background, which could originate from beyond-the-Standard-Model physics. The solar axion is a well-motivated model that has been proposed to explain the excess, though it has tension with astrophysical observations. The axions traveled from the Sun can be absorbed by the electrons in the xenon atoms via the axion-electron coupling. Meanwhile, they can also scatter with the atoms through the inverse Primakoff process via the axion-photon coupling, which emits a photon and mimics the electronic recoil signals. We found that the latter process cannot be neglected. After including the keV photon produced via inverse Primakoff in the detection, the tension with the astrophysical constraints can be significantly reduced. We also explore scenarios involving additional new physics to further alleviate the tension with the astrophysical bounds.

Axions are pseudo-goldstone bosons which naturally arise from the beyond-the-Standard-Model (BSM) physics scenarios [1–3]. Due to an approximate shift symmetry, they can be naturally light. Typically, they are very weakly coupled to other particles, which makes them a good candidate of dark matter or dark sector particles. The phenomenology of the axions is rich and they give unique signals in cosmology, astrophysics, and particle physics [4–8].

XENON1T, a dual-phase Liquid Xenon detector, is one of the leading experiments looking for dark matter. Due to its large volume and low backgrounds, the XENON1T is also sensitive to other rare processes potentially related to the BSM physics. Recently, the XENON1T collaboration reported their searches for low-energy electronic recoil, with an excess in the range of 1-5 keV, which cannot be accounted for by the known backgrounds [9]. The XENON1T collaboration has also performed a fit to the excess using the solar axion model [10]. Since the report from XENON1T collaboration, there have been active speculations about the explanation of the excess [11–38].

It is tempting to explain the XENON1T excess using the solar axions since the axion energy spectrum naturally matches the excess. The axions are produced in the Sun from several processes, including the Primakoff process  $\gamma + Ze \rightarrow Ze + a$ ; the Atomic axion-recombination and de-excitation, Bremsstrahlung, and Compton scattering processes (ABC); and the nuclear transitions. Hence, the axion-photon  $g_{a\gamma}$ , axion-electron  $g_{ae}$  and axion-nucleon  $g_{an}$  couplings enter in the production. With its tiny coupling to photons, the keV axions have a long lifetime and can travel from the Sun to the XENON1T. For the processes in the detector which can give the signal, XENON1T [9] considered only the axion-electron coupling. In this case, the axions could be absorbed by the electrons in xenon atoms.

The relevant axion couplings can be summarized in the

following Lagrangian,

$$\mathcal{L} \supset -g_{ae} \frac{\partial_\mu a}{2m_e} \bar{e} \gamma^\mu \gamma_5 e - \frac{1}{4} g_{a\gamma} a F_{\mu\nu} \tilde{F}^{\mu\nu}. \quad (1)$$

$F^{\mu\nu}$  is the field strength of photon, and its dual  $\tilde{F}^{\mu\nu} = \frac{1}{2} \epsilon^{\mu\nu\alpha\beta} F_{\alpha\beta}$ . However, the parameter space of the solar axion interpretation of the excess is in tension with the astrophysical observations of stellar evolution including the White Dwarfs (WD) and the Horizontal Branch (HB) stars in the globular clusters (GC) [9, 22].

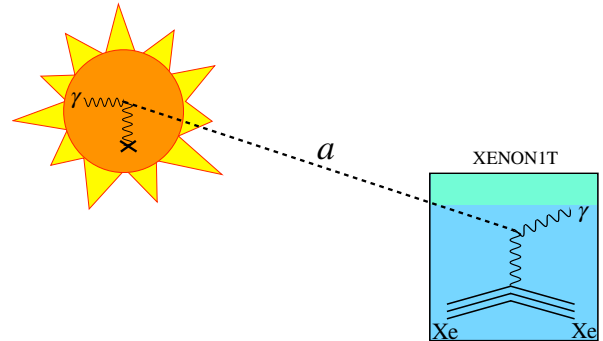


Figure 1. The solar axion induced photon signal through the inverse Primakoff process.

In this letter, we take into account the fact that at keV energy range, the current XENON1T experiment can hardly distinguish the detector response of photons from that of electronic recoils. Hence, instead of electronic recoil, the low-energy photons generated through the inverse Primakoff scattering between solar axion and the xenon atoms in the detector can mimic the electronic signal, as shown in Fig. 1. Using inverse Primakoff process to detect axion is proposed in the cryogenic experiments via Bragg scattering [39–41], and is applied by the SOLAX, COSME, CUORE, CDMS and EDELWEISS

collaborations [42–47]. However, it is not included in the liquid time projection chamber type experiments previously. We show that, after including both the electronic recoil and the inverse Primakoff process, the tension between the solar axion explanation and the astrophysical constraints is significantly reduced.

To further alleviate the astrophysical bounds, we proposed two models: (1)  $U(1)$  Baryon gauge bosons and (2) DM density-dependent interactions. The letter is structured as follows: we first describe the detection using the inverse Primakoff process, and after considering the astrophysics and terrestrial constraints, we present the fit to the data of XENON1T. We then discuss the possible extensions of new physics to further alleviate the tension between the constraints and the XENON1T fit. We conclude in the end.

**Detection from inverse Primakoff process.**— In this section, we compute the contribution to the electronic recoil from the inverse Primakoff process

$$a + \text{Xe} \rightarrow \gamma + \text{Xe},$$

where Xe represents the xenon nucleus. The differential cross section is given by [39, 41, 48]:

$$\frac{d\sigma_{a \rightarrow \gamma}^{\text{invPrim}}}{d\Omega} = \frac{\alpha}{16\pi} g_{a\gamma}^2 \frac{\mathbf{q}^2}{\mathbf{k}^2} (4 - \mathbf{q}^2/\mathbf{k}^2) F_a^2(\mathbf{q}^2), \quad (2)$$

where  $\alpha$  is the fine structure constant,  $\mathbf{k}$  is the momentum of the incoming axion and  $\mathbf{q}$  is the momentum transfer. In the limit of small axion mass,  $m_a \ll |\mathbf{k}|$ , the energy of the outgoing photon is also approximately  $|\mathbf{k}|$ .  $F_a$  is the form factor characterizing the screening effect of the electric charge of the nucleus. It can be written as

$$F_a(\mathbf{q}^2) = Z\mathbf{k}^2/(r_0^{-2} + \mathbf{q}^2), \quad (3)$$

where  $Z = 54$  is the atomic number of xenon and  $r_0$  is the screening length [39], that can be determined numerically. We take eq. (3) and fit the form factors reported in Ref. [49] and obtain  $r_0^{-1} = 4.04 \text{ keV} = (49 \text{ pm})^{-1}$ , which is close to the reciprocal of the xenon atomic radii 108 pm [50].

Next, we calculate the event rate from solar axions with both the inverse Primakoff process and the axioelectric effect. The cross section of the latter process is given by [51, 52]

$$\sigma_{\text{ae}} = \sigma_{\text{pe}} \frac{g_{\text{ae}}^2}{\beta_a} \frac{3E_a^2}{16\pi\alpha m_e^2} \left(1 - \frac{\beta_a^{2/3}}{3}\right), \quad (4)$$

where  $\sigma_{\text{pe}}$  is the photoelectric cross-section [53] and  $\beta_a$  is the axion velocity. We will focus on the low energy excess ( $\lesssim 5 \text{ keV}$ ) throughout this letter, hence only consider the contributions to solar axion flux from the ABC process,  $\Phi_a^{\text{ABC}}$ , and the Primakoff process,  $\Phi_a^{\text{Prim}}$ , and neglect that from nuclear transition of  $^{57}\text{Fe}$ . The ABC flux originates

from the axion-electron coupling and is given by  $\Phi_a^{\text{ABC}} \propto g_{ae}^2$  [54]. The Primakoff flux is given by [55]

$$\frac{d\Phi_a^{\text{Prim}}}{dE_a} = 6 \times 10^{10} \text{ cm}^{-2} \text{ s}^{-1} \text{ keV}^{-1} \times \left(\frac{g_{a\gamma}}{10^{-10} \text{ GeV}}\right)^2 \left(\frac{E_a}{\text{keV}}\right)^{2.481} e^{-E_a/(1.205 \text{ keV})}. \quad (5)$$

Given the solar axion flux  $\Phi_a$ , the differential event rate after including both axioelectric and inverse Primakoff processes in the detection is given by

$$\frac{dR}{dE_r} = \frac{N_A}{A} \left( \frac{d\Phi_a^{\text{ABC}}}{dE}(E_r) + \frac{d\Phi_a^{\text{Prim}}}{dE}(E_r) \right) \times (\sigma_{a \rightarrow \gamma}^{\text{invPrim}}(E_r) + \sigma_{ae}(E_r)), \quad (6)$$

where  $N_A$  is Avogadro constant, and  $E_r$  represents the electronic recoil energy, which is faked by photons in the inverse Primakoff process.

To compare with the results reported by the XENON1T collaboration, we further smear the differential event rate with a Gaussian with its variance satisfying  $\sigma/E_r = a/\sqrt{E_r} + b$ . A numerical fit to the data of XENON1T energy resolution [56] yields  $a = 35.9929 \text{ keV}^{1/2}$  and  $b = -0.2084$ . After the smearing, we apply the detector efficiency [9].

Fig. 2 shows two examples of the differential event rate of the electronic recoils given different values of  $g_{ae}$  and  $g_{a\gamma}$ . In the case that  $g_{ae} = 0$ , the spectrum is only determined by the detection of  $\Phi_a^{\text{Prim}}$  through the inverse Primakoff process. It is clear that with  $g_{ae}$  switched off, solar axions can still account for the low energy excess, although the fit is not as good as that allowing both  $g_{ae}$  and  $g_{a\gamma}$  to be non-zero.

**Constraints from astrophysics and terrestrial experiments.**— The most severe constraints on the solar axion explanation of the XENON1T excess is from the astrophysical observations of the stellar cooling in the HB and red-giant branch (RGB) stars, which we review below.

Axions with sizable  $g_{a\gamma}$  and  $g_{ae}$  couplings speed up the burning of the H-core for RGB and that of the He-core for HB. The lifetime of the stars in the two phases is proportional to their observed numbers. Therefore, one can use the  $R$ -parameter, the ratio of the number of HB stars to that of RGB stars,  $R \equiv N_{\text{HB}}/N_{\text{RGB}}$ , to constrain the stellar cooling due to axions. Ref. [57] reported the averaged  $R$ -parameter over 39 globular clusters with  $R_{\text{av}} = 1.39 \pm 0.03$ . Assuming  $g_{ae} = 0$ ,  $g_{a\gamma}$  is constrained to be  $g_{a\gamma} < 6.6 \times 10^{-11} \text{ GeV}^{-1}$  with 95% C.L. For non-zero  $g_{ae}$ , Ref. [58] presented two theoretical models which give slightly different predictions of the  $R$ -parameter. In Fig. 3, we adopted the resulting 95% C.L. constraints on  $g_{ae} - g_{a\gamma}$  plane for both models from Fig. 4 of [58]. We further discuss the bound dependence on He mass fraction of the globular clusters in the Appendix. The bremsstrahlung energy loss from the

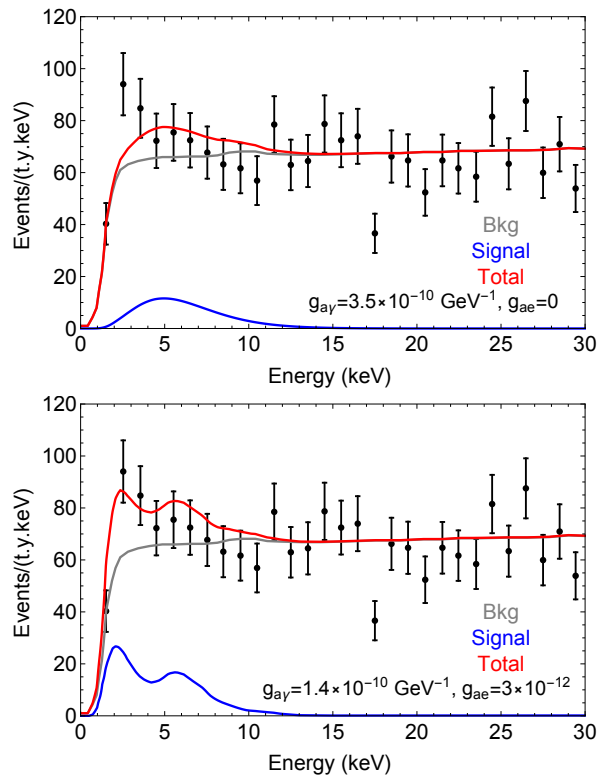


Figure 2. Fit to electronic recoil energy spectrum with  $g_{a\gamma}$  only (top) and both  $g_{a\gamma}$  and  $g_{ae}$  allowed (bottom).

axion-electron coupling affects the white dwarf luminosity function (WDLF) and constrain  $g_{ae} \lesssim 2.8 \times 10^{-13}$  [59]. The same cooling argument on RGB yields a constraint of  $g_{ae} \lesssim 4.3 \times 10^{-13}$  [60]. The global fit of the solar data constrained  $g_{a\gamma} < 4.1 \times 10^{-10} \text{ GeV}^{-1}$  [61]. In Fig. 3, we also show the favored  $g_{ae} - g_{a\gamma}$  parameter region to explain the exotic stellar cooling that hints at a new cooling mechanism beyond the neutrino emission [22, 62].

On the terrestrial experiments side, the axion searches from LUX [63] using axioelectric effect suggest  $g_{ae} < 3.5 \times 10^{-12}$ . Similar constraint is also shown by PandaX [64]. The CAST experiment [65] constrains light axions with  $g_{a\gamma} < 6.6 \times 10^{-11} \text{ GeV}^{-1}$ . But this bound can be significantly weakened if the axion mass is about  $\gtrsim 1 \text{ eV}$ .

**Results.**— In this section, we first present our fit to the XENON1T excess and compare it with the astrophysical constraints, as shown in Fig. 3. We scan two parameters  $g_{ae}$ ,  $g_{a\gamma}$ , and apply the method of least squares to the XENON1T data to find the 90% C.L. contours with (solid red) and without (dashed red) including the inverse Primakoff process. In comparison, we also show the constraints (95% C.L.) from astrophysical observables including WDLF, the tip of RGB, and the  $R$ -parameter (with two models), as well as the constraints from the global fit of the solar data and the direct search at LUX.

From Fig. 3, we see that the inclusion of the inverse-

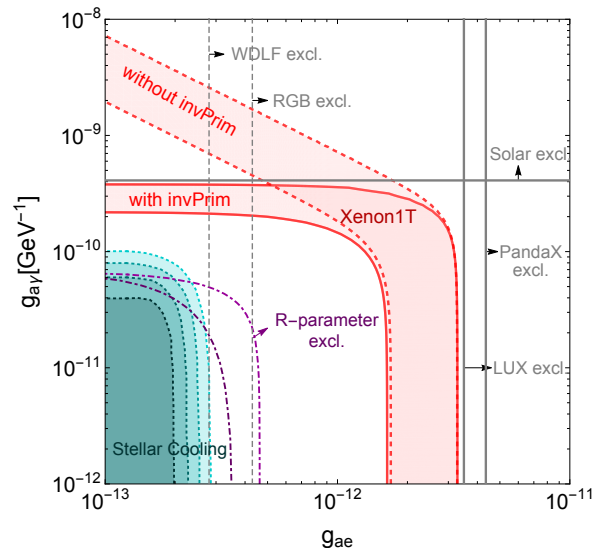


Figure 3. The 2D axion couplings parameter fit for the XENON1T excess after including the inverse Primakoff process. Our best fit (90% C.L.) to the XENON1T excess is shown in the red shaded region with the solid boundary. In comparison, a “XENON-like” analysis with only the electron recoil included as the signal yields a fit shown in the region with the dashed boundary. The main difference is that the inclusion of the inverse Primakoff process allows for a region in which  $g_{a\gamma}$  is relatively large while  $g_{ae}$  can be very small, reducing the tension with the astrophysical data. Also included are the constraints (95% C.L.) from astrophysical observables including WDLF [59], the tip of RGB [60] and the  $R$ -parameter (with two models) [58], as well as the constraints from the global fit of the solar data [61], LUX [63], and PandaX [64], with arrows denoting excluded regions. The shaded green region contains  $1 \sigma$  to  $4 \sigma$  contours favored by the anomalous stellar cooling [22, 62].

Primakoff process has a significant impact on the parameter region preferred by the XENON1T data. In particular, it opens up a parameter region in which  $g_{a\gamma} \gg g_{ae}$  and the inverse Primakoff process gives rise to the observed signal. Moreover, it prefers a  $g_{a\gamma}$  which is in the region of a few  $\times 10^{-10}$ , one order of magnitude smaller than the preferred  $g_{a\gamma}$  without the inclusion of the inverse Primakoff process, satisfying the constraints from the global fit of the solar data, and significantly reducing the tension with the stellar cooling bound.

**Possible extensions.**— From the previous discussion, we see that even though the inclusion of the inverse Primakoff process can significantly improve the prospect of explaining the XENON1T excess with the solar axion, it is still in tension with the stellar cooling bound. If the excess is indeed completely due to new physics, there remains three possibilities. It could certainly come from other new physics instead of the solar axion, in which case a new explanation of the keV scale needs to be found. It is also possible that there is additional uncertainty in the

stellar cooling bound which still has not been appreciated. Instead of pursuing these avenues, we will explore a third possibility. Namely, we introduce new physics in addition to the solar axion to help relax the tension between the XENON1T excess and the stellar cooling bound.

(I) One way to alleviate the astrophysical bound is using axion coupling to both photon and dark gauge boson  $A'$  carrying the  $U(1)_B$  Baryon charge,

$$\mathcal{L} \supset -\frac{1}{2}g_{a\gamma A'}aF'_{\mu\nu}\tilde{F}^{\mu\nu} + g_B A'_\mu J_B^\mu. \quad (7)$$

The  $U(1)_B$   $A'$  couples to Xe nucleus, but not the electrons, such that the form factor suppression from the screening effect of the electric charge of the nucleus is removed, and there is an extra enhancement factor of  $A^2/Z^2$  by coupling to both protons and neutrons. The inverse Primakoff for  $a + N \rightarrow \gamma + N$  is mediated by t-channel  $A'$  and its cross-section is

$$\sigma_{a \rightarrow \gamma}^{A'} = \frac{g_{a\gamma A'}^2 \alpha_B A^2}{8} \frac{(2\eta^2 + 1) \log(4\eta^2 + 1) - 4\eta^2}{\eta^2} F_n^2, \quad (8)$$

where  $\eta = \mathbf{k}/m_{A'}$ ,  $\mathbf{k}$  is the momentum of the axion,  $\alpha_B = g_B^2/4\pi$ ,  $F_n$  is the nuclear form factor which is almost 1 for momentum transfer at keV scale and  $A$  is the number of the nucleons in the nucleus. This cross-section also applies to the Primakoff production of axion flux from HB and Sun. It is proportional to  $A^2$  with  $A'$  mass suppression but no nuclear form factor suppression. Recall that the inverse Primakoff via  $g_{a\gamma}$  is proportional to  $Z^2$ , and after counting the suppression from screening length  $r_0^{-1}$ , the screened charge of Xenon changes to  $Z_{sc} = 5.3$  at  $q = 3$  keV. Given the large  $A = 131$  for xenon, we hope this  $A^2$  can greatly benefit the detection using heavy elements. We found when  $A'$  mass is about  $r_0^{-1}$ , the enhancement in the detector is about its expected form  $A^2/Z^2 \simeq 6$ . When  $m_{A'} < r_0^{-1}$ , the enhancement factor is proportional to  $A^2/Z_{sc}^2$  which is quite large. However, when  $m_{A'} > r_0^{-1}$  there is no enhancement for the detection. The other reason not considering larger  $m_{A'}$  is that the energy loss in star from the Primakoff process will be proportional to  $(\frac{T}{m_{A'}})^4$  for  $m_{A'} \gg T$ . The central region in the Sun is cooler than the core of HB and RGB stars. Therefore, we obtain stronger bounds from the stars in the case of the heavy  $A'$ .

We follow Ref. [48] to calculate the Primakoff induced flux and take the light  $A'$ ,  $m_{A'} = 0.1$  (1) keV, as examples. The energy loss or flux at the HB and Sun is rescaled by 15.6 (8.0) and 16.9 (4.3) times  $\alpha_B g_{a\gamma A'}^2 / (\alpha g_{a\gamma^2})$  comparing with the flux from the  $g_{a\gamma}$  coupling. In both HB and Sun, they are both dominated by hydrogen and helium, therefore the difference between  $Z^2$  and  $A^2$  are not significant. For the detection at XENON1T, the cross-section can be enhanced by about 400 (90) times  $\alpha_B g_{a\gamma A'}^2 / (\alpha g_{a\gamma^2})$ . Therefore, when having the solar axion flux explain the XENON excess, the

energy loss rate from the star could be reduced to 19% (40%). This is able to alleviate the tension between astrophysics and XENON1T excess if  $m_{A'} \lesssim 3$  keV.

Besides  $U(1)_B$ , one can also consider  $U(1)_{B-L}$  by considering the enhancement from neutron number  $(Z - A)$ .

(II) In this second scenario, we consider that if the axion interactions are all assisted with ultralight dark matter  $\phi$ , the bounds can be weakened. The ultralight dark matter assisted interactions are,

$$\mathcal{L} \supset -\frac{\phi}{\Lambda_e} \frac{\partial_\mu a}{2m_e} \bar{e} \gamma^\mu \gamma_5 e - \frac{1}{4} \frac{\phi}{\Lambda_\gamma^2} a F_{\mu\nu} \tilde{F}^{\mu\nu}. \quad (9)$$

The ultralight dark matter has a very large occupation number in the solar system, because its mass is very small e.g.  $m_\phi = 10^{-21}$  eV. Given the relation with local DM density  $\rho_\phi = m_\phi^2 \phi^2/2$ , one can obtain the classical value of the  $\phi$  field which behaves as a vev when there is any DM density. Hence the axion photon and axion gluon coupling are respectively given by  $g_{ae} = \langle \phi \rangle / \Lambda_e \propto \sqrt{\rho_\phi} / \Lambda_e$  and  $g_{a\gamma} = \langle \phi \rangle / \Lambda_\gamma^2 \propto \sqrt{\rho_\phi} / \Lambda_\gamma^2$ . Comparing with the Solar system where the Milky Way (MW) galaxy is abundant of DM ( $\rho_{\text{DM}}^{\text{local}} \sim 0.3 \text{ GeV/cm}^3$ ), the globular clusters (GCs) typically have a lower dark matter mass fraction (e.g.  $f_{\text{DM}} \lesssim 6\%$  for NGC 2419 [66]) comparing to that of MW (84%). Of course, to determine the local DM density around the HB and RGB stars in the 39 GCs that set the  $R$ -parameter constraint, one needs to determine the DM profile of each GC and the location of the stellar populations within them, which is beyond the scope of this paper. But assuming  $\rho_{\text{DM}} = 0.1 \rho_{\text{DM}}^{\text{local}}$  around HB stars in GC allows the coupling on  $g_{a\gamma}$  and  $g_{ae}$  to decrease by a factor of  $\sqrt{10}$ . Using the two theoretical models of the  $R$ -parameter described in the Appendix, this in turn relaxes the constraint on  $g_{a\gamma}$  (assuming  $g_{ae} \lesssim 10^{-13}$ ) from  $g_{a\gamma} < 6.6 \times 10^{-11} \text{ GeV}^{-1}$  to  $g_{a\gamma} < (2 - 3) \times 10^{-10} \text{ GeV}^{-1}$  when adopting the suggested averaged  $R$  value ( $R_{\text{av}} = 1.39 \pm 0.03$ ) and the He abundance ( $Y_{\text{He}} = 0.254 \pm 0.003$ ) from [57]. The favored parameter space to explain the XENON1T excess remain unchanged.

**Conclusions.**— Solar axion is an appealing explanation for the XENON1T excess, with its energy naturally in the keV range. In this letter, we have emphasized the importance of including photon with a similar recoil spectrum as a possible explanation for the XENON1T excess. In particular, it can significantly reduce the tension between the solar axion explanation and the astrophysical data, in particular, the stellar cooling bound. Introducing additional new physics can further alleviate the remaining tension.

We conclude here by briefly discussing future prospects. We expect further sharpening the stellar cooling bound certainly helps to clarify the situation. If there is indeed additional new physics that helps to relieve the tension with the astrophysical bound, it

would be interesting in exploring other possible signals of these new physics. For example, a more sensitive search for the  $U(1)_B$  can have the potential of shedding new light on this scenario. We also note that it is possible to have new physics models in which the photon comes from completely different sources. For example, it can come from a different dark matter scattering process [28] or from decaying from an excited state of the dark matter [23, 37]. In these cases, the spectrum of the photon would be different from the one from the inverse Primakoff process. Future data can be used to distinguishing these scenarios.

**Acknowledgements.**— We would like thank Luca Grandi, Evan Shockley for discussing in detail the response to the electron and photon in the XENON detector and Fei Gao, Jingqiang Ye for the details of fit and the analysis. CG is supported by Fermi Research Alliance, LLC under Contract No. DE-AC02-07CH11359, JL acknowledges support by an Oehme Fellowship, LTW is supported by the DOE grant DE-SC0013642, XPW is supported by the DOE grant DE-AC02-06CH11357, WX is supported by the DOE grant DE-SC0010296, and YZ is supported by the Kavli Institute for Cosmological Physics at the University of Chicago through an endowment from the Kavli Foundation and its founder Fred Kavli.

**Appendix: Dependence of  $R$ -parameter constraints on the He abundance.**— The quickened core-burning process of HB and RGB from axion cooling can be compensated by a larger He abundance. This leads to a degeneracy between the He mass fraction,  $Y_{\text{He}}$ , and the axion couplings,  $g_{ae}$  and  $g_{a\gamma}$  when setting up constraints with observed  $R$  parameter and weakens the coupling constraints when the uncertainties on the He abundance is large.

The determination of  $Y_{\text{He}}$  is particularly challenging for GC due to the absence of the spectroscopic window in the direct detection and the difficulties in stellar simulation.

Given the similar O/H composition between the selected GCs and the low-metallicity HII regions, Ref. [57] uses the  $Y_{\text{He}}$  of the later environment to approximate that of the former one and adopted  $Y_{\text{He}} = 0.254 \pm 0.003$ . Ref. [57] also adopts the He abundance from the Big-Bang nucleosynthesis and that from the early solar system as the lower and higher bounds for  $Y_{\text{He}}$  in GCs.

Ref. [57] updates the theoretical predictions of the  $R$ -parameter by including both the  $g_{ae}$  and  $g_{a\gamma}$  coupling. The two models (labeled as A and B) are given by

$$R_{\text{th}}^A = 6.26Y_{\text{He}} - 0.41 \left( \frac{g_{a\gamma}}{10^{-10} \text{ GeV}^{-1}} \right)^2 - 0.12 - 0.053 \left( \frac{g_{ae}}{10^{-13}} \right)^2 - 1.61\delta\mathcal{M}_c, \quad (10)$$

or

$$R_{\text{th}}^B = 7.33Y_{\text{He}} - 0.095 \sqrt{21.86 + 21.08 \left( \frac{g_{a\gamma}}{10^{-10} \text{ GeV}^{-1}} \right)^2} + 0.02 - 0.053 \left( \frac{g_{ae}}{10^{-13}} \right)^2 - 1.61\delta\mathcal{M}_c, \quad (11)$$

where

$$\delta\mathcal{M}_c = 0.024 \left[ \left( \left( \frac{g_{ae}}{10^{-13}} \right)^2 + 1.23^2 \right)^{\frac{1}{2}} - 1.23 - 0.138 \left( \frac{g_{ae}}{10^{-13}} \right)^{\frac{3}{2}} \right]. \quad (12)$$

In Fig. 4, we showed the resulting 95 % C.L. constraints on the  $g_{ae} - g_{a\gamma}$  plane with the suggested value  $Y_{\text{He}} = 0.255 \pm 0.03$  from the low-metallicity region [57]. To highlight the consequence of  $Y_{\text{He}}$  uncertainty, we also set  $Y_{\text{He}}$  of GCs to that of the primordial He abundance  $Y_{\text{He}} = 0.245 \pm 0.003$  [67] and that of the early Solar system [68],  $Y_{\text{He}} = 0.278 \pm 0.006$ . Note that by approximating  $Y_{\text{He}}$  to the early Solar system value, we assume no chemical evolution occurred during the 8 Gyr between the formation of GC and the Solar system. This is very unlikely.

- 
- [1] R. D. Peccei and H. R. Quinn, “CP Conservation in the Presence of Instantons,” *Phys. Rev. Lett.* **38** (1977) 1440–1443.
  - [2] S. Weinberg, “A New Light Boson?,” *Phys. Rev. Lett.* **40** (1978) 223–226.
  - [3] F. Wilczek, “Problem of Strong  $P$  and  $T$  Invariance in the Presence of Instantons,” *Phys. Rev. Lett.* **40** (1978) 279–282.
  - [4] G. G. Raffelt, “Astrophysical methods to constrain axions and other novel particle phenomena,” *Phys. Rept.* **198** (1990) 1–113.
  - [5] L. D. Duffy and K. van Bibber, “Axions as Dark Matter Particles,” *New J. Phys.* **11** (2009) 105008, [arXiv:0904.3346 \[hep-ph\]](#).
  - [6] M. Kawasaki and K. Nakayama, “Axions: Theory and Cosmological Role,” *Ann. Rev. Nucl. Part. Sci.* **63** (2013) 69–95, [arXiv:1301.1123 \[hep-ph\]](#).
  - [7] D. J. E. Marsh, “Axion Cosmology,” *Phys. Rept.* **643** (2016) 1–79, [arXiv:1510.07633 \[astro-ph.CO\]](#).
  - [8] P. W. Graham, I. G. Irastorza, S. K. Lamoreaux, A. Lindner, and K. A. van Bibber, “Experimental Searches for the Axion and Axion-Like Particles,” *Ann. Rev. Nucl. Part. Sci.* **65** (2015) 485–514, [arXiv:1602.00039 \[hep-ex\]](#).
  - [9] XENON Collaboration, E. Aprile *et al.*, “Observation of Excess Electronic Recoil Events in XENON1T,” [arXiv:2006.09721 \[hep-ex\]](#).
  - [10] K. van Bibber, P. M. McIntyre, D. E. Morris, and G. G. Raffelt, “A Practical Laboratory Detector for Solar Axions,” *Phys. Rev.* **D39** (1989) 2089.
  - [11] F. Takahashi, M. Yamada, and W. Yin, “XENON1T anomaly from anomaly-free ALP dark matter and its

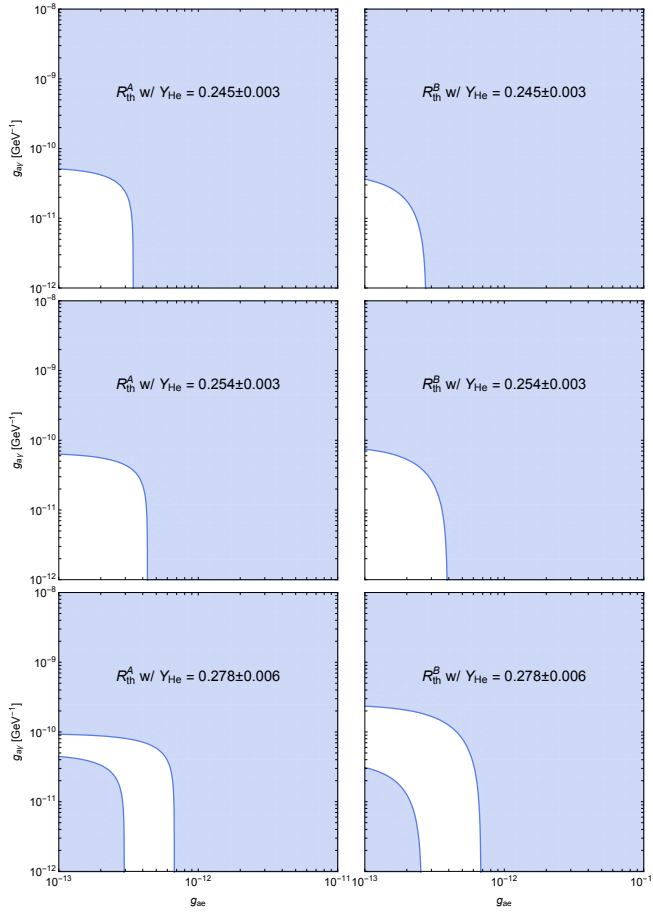


Figure 4. 95% C.L. excluded parameter space (shaded with blue) from the ratio of the number of HB stars to that of RGB stars in GCs. Here we adopted the averaged  $R_{av} = 1.39 \pm 0.03$  and considered the theoretical models of Eq. (10) (left) and Eq. (11) (right). We approximate the  $Y_{He}$  value from the primordial He abundance (upper), the low-metallicity region (middle), and the early Solar system (lower).

implications for stellar cooling anomaly,” [arXiv:2006.10035 \[hep-ph\]](#).

- [12] C. A. O’Hare, A. Caputo, A. J. Millar, and E. Vitagliano, “Axion helioscopes as solar magnetometers,” [arXiv:2006.10415 \[astro-ph.CO\]](#).
- [13] K. Kannike, M. Raidal, H. Veermäe, A. Strumia, and D. Teresi, “Dark Matter and the XENON1T electron recoil excess,” [arXiv:2006.10735 \[hep-ph\]](#).
- [14] d. Amaral, Dorian Warren Praia, D. G. Cerdeno, P. Foldenauer, and E. Reid, “Solar neutrino probes of the muon anomalous magnetic moment in the gauged  $U(1)_{L\mu-L\tau}$ ,” [arXiv:2006.11225 \[hep-ph\]](#).
- [15] G. Alonso-Álvarez, F. Ertas, J. Jaeckel, F. Kahlhoefer, and L. Thormaehlen, “Hidden Photon Dark Matter in the Light of XENON1T and Stellar Cooling,” [arXiv:2006.11243 \[hep-ph\]](#).
- [16] B. Fornal, P. Sandick, J. Shu, M. Su, and Y. Zhao, “Boosted Dark Matter Interpretation of the XENON1T Excess,” [arXiv:2006.11264 \[hep-ph\]](#).
- [17] C. Boehm, D. G. Cerdeno, M. Fairbairn, P. A. Machado, and A. C. Vincent, “Light new physics in XENON1T,” [arXiv:2006.11250 \[hep-ph\]](#).
- [18] K. Harigaya, Y. Nakai, and M. Suzuki, “Inelastic Dark Matter Electron Scattering and the XENON1T Excess,” [arXiv:2006.11938 \[hep-ph\]](#).
- [19] A. Bally, S. Jana, and A. Trautner, “Neutrino self-interactions and XENON1T electron recoil excess,” [arXiv:2006.11919 \[hep-ph\]](#).
- [20] L. Su, W. Wang, L. Wu, J. M. Yang, and B. Zhu, “Xenon1T anomaly: Inelastic Cosmic Ray Boosted Dark Matter,” [arXiv:2006.11837 \[hep-ph\]](#).
- [21] M. Du, J. Liang, Z. Liu, V. Q. Tran, and Y. Xue, “On-shell mediator dark matter models and the Xenon1T anomaly,” [arXiv:2006.11949 \[hep-ph\]](#).
- [22] L. Di Luzio, M. Fedele, M. Giannotti, F. Mescia, and E. Nardi, “Solar axions cannot explain the XENON1T excess,” [arXiv:2006.12487 \[hep-ph\]](#).
- [23] N. F. Bell, J. B. Dent, B. Dutta, S. Ghosh, J. Kumar, and J. L. Newstead, “Explaining the XENON1T excess with Luminous Dark Matter,” [arXiv:2006.12461 \[hep-ph\]](#).
- [24] Y. Chen, J. Shu, X. Xue, G. Yuan, and Q. Yuan, “Sun Heated MeV-scale Dark Matter and the XENON1T Electron Recoil Excess,” [arXiv:2006.12447 \[hep-ph\]](#).
- [25] D. Aristizabal Sierra, V. De Romeri, L. Flores, and D. Papoulias, “Light vector mediators facing XENON1T data,” [arXiv:2006.12457 \[hep-ph\]](#).
- [26] J. Buch, M. A. Buen-Abad, J. Fan, and J. S. C. Leung, “Galactic Origin of Relativistic Bosons and XENON1T Excess,” [arXiv:2006.12488 \[hep-ph\]](#).
- [27] G. Choi, M. Suzuki, and T. T. Yanagida, “XENON1T Anomaly and its Implication for Decaying Warm Dark Matter,” [arXiv:2006.12348 \[hep-ph\]](#).
- [28] G. Paz, A. A. Petrov, M. Tammaro, and J. Zupan, “Shining dark matter in Xenon1T,” [arXiv:2006.12462 \[hep-ph\]](#).
- [29] U. K. Dey, T. N. Maity, and T. S. Ray, “Prospects of Migdal Effect in the Explanation of XENON1T Electron Recoil Excess,” [arXiv:2006.12529 \[hep-ph\]](#).
- [30] A. N. Khan, “Can nonstandard neutrino interactions explain the XENON1T spectral excess?,” [arXiv:2006.12887 \[hep-ph\]](#).
- [31] Q.-H. Cao, R. Ding, and Q.-F. Xiang, “Exploring for sub-MeV Boosted Dark Matter from Xenon Electron Direct Detection,” [arXiv:2006.12767 \[hep-ph\]](#).
- [32] R. Primulando, J. Julio, and P. Uttayarat, “Collider Constraints on a Dark Matter Interpretation of the XENON1T Excess,” [arXiv:2006.13161 \[hep-ph\]](#).
- [33] K. Nakayama and Y. Tang, “Gravitational Production of Hidden Photon Dark Matter in light of the XENON1T Excess,” [arXiv:2006.13159 \[hep-ph\]](#).
- [34] H. M. Lee, “Exothermic Dark Matter for XENON1T Excess,” [arXiv:2006.13183 \[hep-ph\]](#).
- [35] G. B. Gelmini, V. Takhistov, and E. Vitagliano, “Scalar Direct Detection: In-Medium Effects,” [arXiv:2006.13909 \[hep-ph\]](#).
- [36] Y. Jho, J.-C. Park, S. C. Park, and P.-Y. Tseng, “Gauged Lepton Number and Cosmic-ray Boosted Dark Matter for the XENON1T Excess,” [arXiv:2006.13910 \[hep-ph\]](#).
- [37] M. Baryakhtar, A. Berlin, H. Liu, and N. Weiner, “Electromagnetic Signals of Inelastic Dark Matter Scattering,” [arXiv:2006.13918 \[hep-ph\]](#).
- [38] H. An, M. Pospelov, J. Pradler, and A. Ritz, “New



- limits on dark photons from solar emission and keV scale dark matter,” [arXiv:2006.13929 \[hep-ph\]](#).
- [39] W. Buchmuller and F. Hoogeveen, “Coherent Production of Light Scalar Particles in Bragg Scattering,” *Phys. Lett.* **B237** (1990) 278–283.
- [40] E. A. Paschos and K. Zioutas, “A Proposal for solar axion detection via Bragg scattering,” *Phys. Lett.* **B323** (1994) 367–372.
- [41] R. J. Creswick, F. T. Avignone, III, H. A. Farach, J. I. Collar, A. O. Gattone, S. Nussinov, and K. Zioutas, “Theory for the direct detection of solar axions by coherent Primakoff conversion in germanium detectors,” *Phys. Lett.* **B427** (1998) 235–240, [arXiv:hep-ph/9708210 \[hep-ph\]](#).
- [42] **SOLAX** Collaboration, F. T. Avignone, III *et al.*, “Experimental search for solar axions via coherent Primakoff conversion in a germanium spectrometer,” *Phys. Rev. Lett.* **81** (1998) 5068–5071, [arXiv:astro-ph/9708008 \[astro-ph\]](#).
- [43] **COSME** Collaboration, A. Morales *et al.*, “Particle dark matter and solar axion searches with a small germanium detector at the Canfranc Underground Laboratory,” *Astropart. Phys.* **16** (2002) 325–332, [arXiv:hep-ex/0101037 \[hep-ex\]](#).
- [44] **CUORE** Collaboration, C. Arnaboldi *et al.*, “CUORE: A Cryogenic underground observatory for rare events,” *Nucl. Instrum. Meth.* **A518** (2004) 775–798, [arXiv:hep-ex/0212053 \[hep-ex\]](#).
- [45] **CUORE** Collaboration, C. Arnaboldi *et al.*, “Physics potential and prospects for the CUORICINO and CUORE experiments,” *Astropart. Phys.* **20** (2003) 91–110, [arXiv:hep-ex/0302021 \[hep-ex\]](#).
- [46] **CDMS** Collaboration, Z. Ahmed *et al.*, “Search for Axions with the CDMS Experiment,” *Phys. Rev. Lett.* **103** (2009) 141802, [arXiv:0902.4693 \[hep-ex\]](#).
- [47] E. Armengaud *et al.*, “Axion searches with the EDELWEISS-II experiment,” *JCAP* **1311** (2013) 067, [arXiv:1307.1488 \[astro-ph.CO\]](#).
- [48] G. Raffelt, *Stars as laboratories for fundamental physics: The astrophysics of neutrinos, axions, and other weakly interacting particles*, 5, 1996.
- [49] E. N. M. M. A. O. P. J. Brown, A. G. Fox and B. T. M. Willis, “Chapter 6.1. intensity of diffracted intensities,” *International Tables for Crystallography C*, **ch. 6.1** (2006) 554–595. <https://it.iucr.org/Cb/ch6o1v0001/>.
- [50] E. Clementi, D. L. Raimondi, and W. P. Reinhardt, “Atomic screening constants from scf functions. ii. atoms with 37 to 86 electrons,” *The Journal of Chemical Physics* **47** no. 4, (1967) 1300–1307.
- [51] M. Pospelov, A. Ritz, and M. B. Voloshin, “Bosonic super-WIMPs as keV-scale dark matter,” *Phys. Rev.* **D78** (2008) 115012, [arXiv:0807.3279 \[hep-ph\]](#).
- [52] **CUORE** Collaboration, F. Alessandria *et al.*, “Search for 14.4 keV solar axions from M1 transition of Fe-57 with CUORE crystals,” *JCAP* **1305** (2013) 007, [arXiv:1209.2800 \[hep-ex\]](#).
- [53] K. Arisaka, P. Beltrame, C. Ghag, J. Kaidi, K. Lung, A. Lyashenko, R. D. Peccei, P. Smith, and K. Ye, “Expected Sensitivity to Galactic/Solar Axions and Bosonic Super-WIMPs based on the Axio-electric Effect in Liquid Xenon Dark Matter Detectors,” *Astropart. Phys.* **44** (2013) 59–67, [arXiv:1209.3810 \[astro-ph.CO\]](#).
- [54] J. Redondo, “Solar axion flux from the axion-electron coupling,” *JCAP* **1312** (2013) 008, [arXiv:1310.0823 \[hep-ph\]](#).
- [55] B. B. Markus Kuster, Georg Raffelt, *Axions*. Springer-Verlag Berlin Heidelberg, 2008.
- [56] **XENON** Collaboration, E. Aprile *et al.*, “Observation of two-neutrino double electron capture in  $^{124}\text{Xe}$  with XENONIT,” *Nature* **568** no. 7753, (2019) 532–535, [arXiv:1904.11002 \[nucl-ex\]](#).
- [57] A. Ayala, I. Domínguez, M. Giannotti, A. Mirizzi, and O. Straniero, “Revisiting the bound on axion-photon coupling from Globular Clusters,” *Phys. Rev. Lett.* **113** no. 19, (2014) 191302, [arXiv:1406.6053 \[astro-ph.SR\]](#).
- [58] M. Giannotti, I. Irastorza, J. Redondo, and A. Ringwald, “Cool WISPs for stellar cooling excesses,” *JCAP* **05** (2016) 057, [arXiv:1512.08108 \[astro-ph.HE\]](#).
- [59] M. M. Miller Bertolami, B. E. Melendez, L. G. Althaus, and J. Isern, “Revisiting the axion bounds from the Galactic white dwarf luminosity function,” *JCAP* **1410** (2014) 069, [arXiv:1406.7712 \[hep-ph\]](#).
- [60] N. Viaux, M. Catelan, P. B. Stetson, G. Raffelt, J. Redondo, A. A. R. Valcarce, and A. Weiss, “Neutrino and axion bounds from the globular cluster M5 (NGC 5904),” *Phys. Rev. Lett.* **111** (2013) 231301, [arXiv:1311.1669 \[astro-ph.SR\]](#).
- [61] N. Vinyoles, A. Serenelli, F. L. Villante, S. Basu, J. Redondo, and J. Isern, “New axion and hidden photon constraints from a solar data global fit,” *JCAP* **1510** (2015) 015, [arXiv:1501.01639 \[astro-ph.SR\]](#).
- [62] M. Giannotti, I. G. Irastorza, J. Redondo, A. Ringwald, and K. Saikawa, “Stellar Recipes for Axion Hunters,” *JCAP* **10** (2017) 010, [arXiv:1708.02111 \[hep-ph\]](#).
- [63] **LUX** Collaboration, D. S. Akerib *et al.*, “First Searches for Axions and Axionlike Particles with the LUX Experiment,” *Phys. Rev. Lett.* **118** no. 26, (2017) 261301, [arXiv:1704.02297 \[astro-ph.CO\]](#).
- [64] **PandaX** Collaboration, C. Fu *et al.*, “Limits on Axion Couplings from the First 80 Days of Data of the PandaX-II Experiment,” *Phys. Rev. Lett.* **119** no. 18, (2017) 181806, [arXiv:1707.07921 \[hep-ex\]](#).
- [65] K. Barth *et al.*, “CAST constraints on the axion-electron coupling,” *JCAP* **05** (2013) 010, [arXiv:1302.6283 \[astro-ph.SR\]](#).
- [66] R. Ibata, C. Nipoti, A. Sollima, M. Bellazzini, S. Chapman, and E. Dalessandro, “Do globular clusters possess Dark Matter halos? A case study in NGC 2419,” *Mon. Not. Roy. Astron. Soc.* **428** (2013) 3648, [arXiv:1210.7787 \[astro-ph.CO\]](#).
- [67] **Particle Data Group** Collaboration, M. Tanabashi *et al.*, “Review of Particle Physics,” *Phys. Rev.* **D98** no. 3, (2018) 030001.
- [68] K. M. Serenelli and S. Basu, “Determining the initial helium abundance of the sun,” *The Astrophysical Journal* **719** no. 1, (Jul, 2010) 865–872. <http://dx.doi.org/10.1088/0004-637X/719/1/865>.